



Examination of Helicopter Dynamic Response Using Dynamic Inflow Model

F. Shahmiri*, Y. Sarafraz

Aerospace Department, Malek Ashtar University of Technology, Tehran, Iran

ABSTRACT: This paper concerned with the examination of on-axis and off-axis dynamic responses of helicopters using a dynamic induced velocity model for a main rotor. The model consisted a canonical Legendry polynomial and a trigonometric function with a time dependent coefficients and arbitrary harmonics. The main reason for this, was the compatibility of the Legendry polynomial with the potential acceleration function presented by Laplace PDE for a main rotor at incompressible flow condition. The novel of the present research is the inflow dynamics with finite state wake that was efficiently adopted with the dynamic equations of single main rotor helicopters in the time domain. Therefore, the discretization of the wake inflow was avoided by the definition of finite inflow states. Furthermore, the possibility of air load computations is achieved through the state formulation and quasi steady aerodynamic implementation. Moreover, the singularity problem associated with the traditional inflow dynamics was avoided through the current inflow state. The obtained results showed that using dynamic inflow model with 28-states and 4-harmonics significantly improves the off-axis dynamic responses of single main rotor helicopters. Comparison of results with the flight-test data and with the showed that both the off-axis and on-axis response of helicopters experience a fairly good improvements.

Review History:

Received: 13 March 2016
Revised: 25 July 2016
Accepted: 23 October 2016
Available Online: 10 November 2016

Keywords:

Helicopter
Main rotor
Dynamic induced velocity
Dynamic simulation

1- Introduction

Generally, helicopter flight dynamics simulation is the task of analyzing the dynamic response of a helicopter as a whole, particularly, helicopter response during unsteady transient conditions. The flight dynamics analysis inherently involves three fundamental sections. The first section is to describe the dynamics of the various components of the helicopter in an appropriate mathematical form. The second element involves the coupling of each component to form a complete model describing the dynamics of the helicopter as a whole. The third section is to use this complete model for determination of trim equilibrium conditions and time history responses to arbitrary pilot control inputs.

Although some significant efforts made around for a number of years have been slightly promoted the dynamic responses of helicopters, the reports show a long-term occurrence that described the off-axis problem as a major disruption in explanation of the final results [1-3]. This probably means that the most of the former studies are somewhat sophisticated when compared to real flights.

In the present work, more sophisticated representation of the main rotor dynamics and aerodynamics leading to improve both the on-axis and off-axis response is described. This is a cause of merging the coupled flap-lag and torsion elastic blade model along with an unsteady finite state inflow model in this research. The finite-state inflow theory improves the former Pitt-Peters inflow model by entering a higher-order representation of inflow variation along the rotor radius and higher-harmonic variations around the azimuth. The type of result that is of our interest is the inclusion of higher-harmonic blade loadings and higher-frequency loads on the helicopter during hover and forward flight phase. Fig. 1 shows

a general layout of the finite state wake model formation. While the normal induced velocity is the most significant of all other components, the reduced ODEs corresponded to the third component of inflow vector is adequate for inflow calculations.

2- Methodology

The solution of the normal inflow ODEs is obtained when the forcing function together with normal induced velocity is approximated by a set of radial modal functions (Legendre polynomial) and azimuth-wise harmonics as [6]:

$$V_i(x, \psi, t) = \sum_{r=0}^{\infty} \sum_{j=r+1, r+3, \dots}^{\infty} \varphi_j^r(x) [\alpha_j^r(t) \cos(r\psi) + \beta_j^r(t) \sin(r\psi)] \quad (1)$$

Where:

$$\varphi_m^n(x) = \sqrt{(2n+1)H_n^m} \sum_{q=m, m+2, \dots}^{n-1} x^q (-1)^{\frac{q-m}{2}} B$$

$$B = \frac{(m+q)!!}{(q-m)!!(q+m)!!(m-q-1)!!} \quad (2)$$

$$H_n^m = \frac{(n+m-1)!!(n-m-1)!!}{(n+m)!!(n-m)!!}$$

The number of inflow states is obtained through the use of the following differential equations defined in the tip path plane coordinate system as:

$$\begin{bmatrix} \ddots & & & \\ & K_n^m & & \\ & & \ddots & \\ & & & \ddots \end{bmatrix} \begin{Bmatrix} \dot{\alpha}_j^r \\ \alpha_j^r \end{Bmatrix} + \mathcal{V} \hat{L}_{jn}^{mc} \begin{Bmatrix} \dot{\alpha}_j^r \\ \alpha_j^r \end{Bmatrix} = \begin{Bmatrix} \tau_n^{mc} \\ \tau_n^{mc} \end{Bmatrix}$$

$$\begin{bmatrix} \dots \\ K_n^m \\ \dots \end{bmatrix} \{ \beta_j^r \} + 2\mathcal{V} \left[\hat{L}_{jn}^{ms} \right]^{-1} \{ \beta_j^r \} = \{ \tau_n^{ms} \} \quad (3)$$

where cosine harmonic coupling matrices are [2]:

$$\begin{aligned} \hat{L}_{jn}^{mc} &= (E)^m [\Gamma_{jn}^{rm}] \\ \hat{L}_{jn}^{rc} &= (E)^{|m-r|} + (-1)^s E^{|m+r|} [\Gamma_{jn}^{rm}] \\ \hat{L}_{jn}^{ms} &= (E)^{|m-r|} - (-1)^s E^{|m+r|} [\Gamma_{jn}^{rm}] \\ E &= \tan|\chi/2| \quad (0 \leq \chi \leq \frac{\pi}{2}) \end{aligned} \quad (4)$$

Furthermore, the pressure coefficients τ_n^{mc} and τ_n^{ms} in Eq. (3) correspond to the lift distribution through the following equations;

$$\begin{aligned} \tau_n^{0c} &= \frac{1}{2\pi} \sum_{i=1}^N \left[\int_e^1 L_i \phi_n^0(\hat{x}) d\hat{x} \right] \\ \tau_n^{mc} &= \frac{1}{\pi} \sum_{i=1}^N \left[\int_e^1 L_i \phi_n^m(\hat{x}) \cos(m\psi_i) d\hat{x} \right] \\ \tau_n^{ms} &= \frac{1}{\pi} \sum_{i=1}^N \left[\int_e^1 L_i \phi_n^m(\hat{x}) \sin(m\psi_i) d\hat{x} \right] \end{aligned} \quad (5)$$

where [4]:

$$L_i = \begin{bmatrix} \cos(\cos \beta_{lc} + \sin \beta_{ls}) \\ 0 \\ \sin(\cos \beta_{lc} + \sin \beta_{ls}) \end{bmatrix} (F_A)^U \quad (6)$$

Fig. 1 showed:

$$(F_A)^L = \frac{1}{2} \rho c v \begin{bmatrix} C_d v_1 - C_l v_2 \cos \gamma_l \\ \frac{C_l v_1}{\cos \gamma_l} + C_d v_2 \\ \frac{C_l v_2 v_3 \cos \gamma_l}{v_1} + C_d v_3 \end{bmatrix} \quad (7)$$

3- Results and Discussion

In this section, the transient responses of an articulated rotor helicopter to step-inputs at various trim conditions have been calculated, and compared with flight test data [5]. The test data used for the comparison were obtained in a series of tests conducted for use in validation of the Rotorcraft Systems Integration Simulator. The trim data and selected transient-response time histories were provided to Sikorsky for use in their validation of the mathematical models. No stability augmentation was used during transient-response data acquisitions. Analog and digital stability augmentation systems, the flight path stabilization system, and the horizontal stabilizer control system were disabled. This is a highly degraded configuration; the results are not

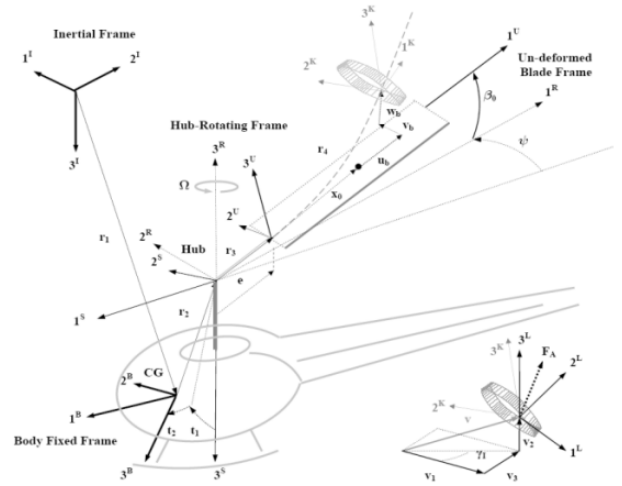


Figure 1. Schematic of helicopter coordinate systems

representative of the UH-60A in the normal operation. The test procedure normally consisted of stabilizing in trim with one of the two redundant stability augmentation systems on; this was disabled one second before the control input. Unsatisfactory stability characteristics of the un-augmented aircraft, especially in pitch, required the pilot to initiate recovery within a few seconds of the input for the reasons of instability or safety. Furthermore, because the test program was organized in order to provide standard handling qualities data, the presented results are focused on both off-axis and on-axis dynamic response. Validations are discussed in terms of the pitch, roll, and yaw rate responses, which are important from the handling qualities point of view.

In all cases, trim control settings are normally obtained from the previous section for hover and 50-knot forward flight speed, corresponding to advanced ratios equaled to 0 and 0.11, respectively. All results are taken at an altitude of 3000 feet in a standard atmosphere and a gross weight of 16,000 lb. This corresponds to a blade loading of 0.069.

As can be seen from Fig. 2, the blade modeling, changing from second to 6th natural modes shapes, has very little influence on the prediction of power required.

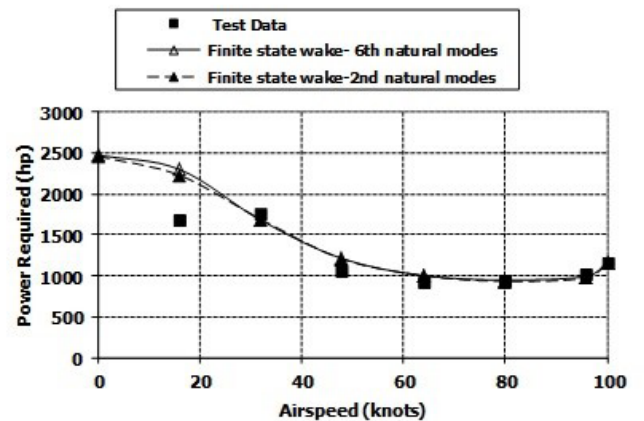


Figure 2. Effect of blade modeling on helicopter power required versus airspeed

In Fig. 3 pitch rate responses to lateral cyclic input for trimmed flight condition at 50 knots forward speed are shown. The

time-history plots show that the finite state off-axis pitch rate response reaches to a maximum value, corresponding to -0.56 degree per second, at which the control and damping moment balances, but with a different sign and magnitude compared to flight test data. The calculated pitch response indicates that the off-axis pitch response still suffers from a problem. This is likely due to the sign of the restoring moment and the helicopter translational acceleration, which strongly depends on the induced inflow distribution over the rotor disc. It seems that there is a phase shift in predicted finite state result in comparison with flight test data. This is due to the low-frequency nature of the finite state inflow modeling in which it is assumed that the main rotor aerodynamics occurs slowly. Results show that the off-axis yaw rate response weakly depends on the type of implemented inflow models.

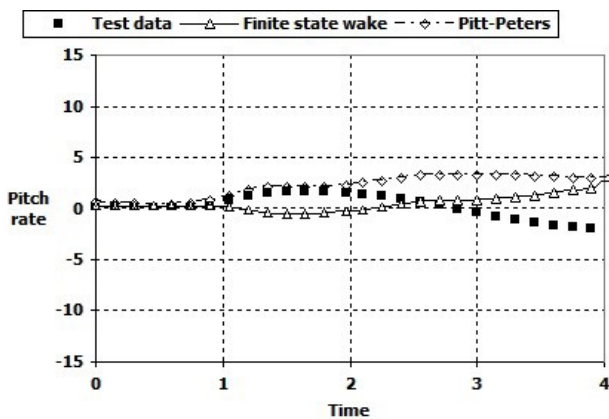


Figure 3. Off-axis pitch rate responses to lateral cyclic input, forward flight.

4- Conclusions

The practical implementation of the three-dimensional unsteady induced inflow model, a finite state representation, is included in a comprehensive flight dynamic simulation program. Based on the results presented in this paper, the

following conclusions can be drawn; the on-axis responses are not significantly affected by inflow modeling in the time range of interest for flight dynamics applications, and correlations with flight test data are generally good. The finite state inflow model, which does not include induced wake distortions, shows fairly good predictions of the off-axis responses. The addition of the finite state inflow model fairly improves the off-axis response predictions both quantitatively and qualitatively.

References

- [1] J. Zhao, J. V. R. Prasad, D. A. Peters Rotor Dynamic Wake Distortion Model for Helicopter Maneuvering Flight, *Journal of the American Helicopter Society*, 49(4) (2004) 414–424.
- [2] D. Fusato, R. Celi, Multidisciplinary Design Optimization for Helicopter Aeromechanics and Handling Qualities, *Journal of Aircraft*, 43(1) (2006) 241-252.
- [3] F. Shahmiri, F. Saghafi, Improvement of Dynamic Response Prediction of Helicopters, *Journal of Aircraft Engineering and Aerospace Technology*, 79(76) (2007) 579-592.
- [4] D. M. Pitt, D.A. Peters, (1981), Theoretical Prediction of Dynamic Inflow Derivatives, *Vertica*, 5(1) (1981) 21-34.
- [5] R. Gori, F. Pausilli, M. D. Pavel, State-space rotor aeroelastic modeling for real-time helicopter flight simulation,” *Advanced Material Research*, 10(16) (2014) 451–459.
- [6] Zhao, Jinggen, He, Chengjian, A Finite State Dynamic Wake Model Enhanced with Vortex Particle Method–Derived Modeling Parameters for Coaxial Rotor Simulation and Analysis, 61(2)(2016) 1-9.
- [7] M. G. Ballin, M. A. Dalang-Secretan, Validation of the Dynamic Response of a Blade-Element UH-60 Simulation Model in Hovering Flight, *Proceedings of the American Helicopter Society 46th Annual Forum*, Washington D.C. (1990).

Please cite this article using:

F. Shahmiri and Y. Sarafraz, Examination of Helicopter Dynamic Response Using Dynamic Inflow Model, *Amirkabir J. Mech. Eng.*, 50(1) (2018) 189-196.
DOI: 10.22060/mej.2016.806



